

# Maculas Affected by Age-Related Macular Degeneration Contain Increased Chelatable Iron in the Retinal Pigment Epithelium and Bruch's Membrane

Paul Hahn; Ann H. Milam, PhD; Joshua L. Dunaief, MD, PhD

**Objective:** To investigate whether iron is involved in the pathogenesis of age-related macular degeneration (AMD).

**Methods:** Postmortem AMD-affected (nonexudative or exudative) and healthy maculas were studied using the 3,3'-diaminobenzidine-enhanced Perls Prussian blue stain. The Perls Prussian blue stain was quantified by computer-assisted analysis of digital images. To determine whether the iron was chelatable, sections treated with the iron chelator deferoxamine were compared with adjacent, nonchelated sections.

**Results:** Compared with healthy maculas, AMD-affected maculas had statistically significant increases in the total iron level. Some of this iron was chelatable. The iron was present in retinal pigment epithelium and Bruch's membrane in maculas from patients who had drusen only, geographic atrophy, and exudative AMD

in pathologic areas and, occasionally, in relatively healthy areas.

**Conclusions:** Oxidative stress has been implicated in the pathogenesis of AMD by the Age-Related Eye Disease Study. Increased concentrations of iron, which generate highly reactive hydroxyl radicals via the Fenton reaction, may induce oxidative stress in the macula and lead to AMD. As the increased iron concentrations in AMD-affected eyes consist in part of a chelatable iron pool, treatment of patients who have AMD with iron chelators might be considered a potential therapy. While there are, as yet, no clinical data indicating that the treatment of patients who have AMD with iron chelators is beneficial, data presented herein indicate that further investigation of iron concentrations in postmortem tissues and the mechanisms of iron transport in the retina is warranted.

*Arch Ophthalmol.* 2003;121:1099-1105

**A**GE-RELATED macular degeneration (AMD), a degenerative disorder of the macula, is the most common cause of irreversible blindness in the United States in individuals older than 65 years.<sup>1</sup> The early stage of AMD is characterized clinically by large, soft drusen and pigmentary abnormalities of the retinal pigment epithelium (RPE) and retina. As the course of AMD advances, choroidal neovascularization can be observed in wet or exudative AMD, or large areas of geographic atrophy (GA) can occur in the more common dry form.

While the natural history of AMD has been described, its pathogenesis is unknown. There is growing evidence that oxidative stress and free radical damage play a pivotal role in inducing AMD.<sup>2</sup> In the Age-Related Eye Disease Study, a large, multicenter clinical trial, dietary supplementation with antioxidants and zinc significantly reduced development of ad-

vanced AMD.<sup>3</sup> While these data implicate oxidative stress in the pathogenesis of AMD, the source of damaging reactive oxygen species is unknown.

Iron, a known source of free radicals, reacts in its ferrous (II) state with hydrogen peroxide (H<sub>2</sub>O<sub>2</sub>) in the Fenton reaction to produce highly reactive hydroxyl radicals. A recent study of another age-related neurodegenerative disease, Alzheimer disease, demonstrated increased iron concentrations in senile plaques and neurofibrillary tangles of postmortem brains compared with healthy brains.<sup>4</sup> To investigate whether iron might be involved in the pathogenesis of AMD, we documented the distribution of iron in maculas with nonexudative AMD (GA or early AMD) or exudative AMD compared with healthy maculas. We found that AMD-affected maculas have statistically significantly increased total iron concentrations, including a pool of chelatable iron, in the RPE and Bruch's membrane. These

*From the F. M. Kirby Center for Molecular Ophthalmology, Scheie Eye Institute, University of Pennsylvania, Philadelphia. The authors have no relevant financial interest in this article.*

findings suggest that iron may contribute to oxidative damage in AMD.

## METHODS

### SOURCE OF TISSUE AND POPULATION PROFILE

Postmortem eyes were obtained through the Foundation Fighting Blindness, Owings Mills, Md, eye donor program, the National Disease Research Interchange, Philadelphia, Pa, and directly through eye banks. The pathology reports provided for some of the patients the age, sex, brief ocular and medical histories, cause of death, and postmortem interval. The 12 healthy eye donors consisted of 6 men, 4 women, and 2 donors whose sexes were not designated. The mean age was 77.3 years (age range, 65-95 years); the mean postmortem interval was 9.8 hours (range, 2.0-30 hours). The 12 AMD-affected eye donors consisted of 3 men, 3 women, and 6 donors whose sexes were not designated. The mean age was 77.1 years (age range, 66-94 years); the mean postmortem interval was 12.0 hours (range, 5-29 hours). The AMD group consisted of 4 eyes with exudative AMD and 8 eyes with nonexudative AMD. Among the nonexudative AMD-affected eyes, 5 had GA and 3 had drusen and only minimal photoreceptor and RPE atrophy (early AMD). Two donors with AMD had potentially relevant comorbid conditions. One had glaucoma and another had diabetes mellitus, but neither had exceptional Perls Prussian blue staining compared with other AMD-affected eyes. The histopathologic studies followed the tenets of the Declaration of Helsinki, and informed consent was obtained from all eye donors before death. Approval for research on human postmortem donor eyes was obtained from the University of Pennsylvania, Philadelphia.

### TISSUE PROCESSING

After enucleation, a small incision was made in the pars plana and each eye was fixed in a combination of 4% paraformaldehyde and 0.5% glutaraldehyde in 0.1M phosphate-buffer solution for several days. The fixed eyes were transferred to 2% paraformaldehyde for storage. A block of tissue ranging from 1 to 1.5 cm long and 0.5 cm wide containing the optic disc and macula was processed as serial 5- $\mu$ m-thick paraffin sections or as 10- $\mu$ m-thick cryosections as previously described.<sup>5</sup>

### IRON HISTOCHEMICAL DETECTION

Sections were stained with Perls Prussian blue for iron by incubation in a combination of 5% potassium ferrocyanide in 5% aqueous hydrochloric acid for 30 minutes at room temperature, yielding a Perls Prussian blue reaction product. Sensitivity for iron detection was enhanced by subsequent incubation in 0.75 mg/mL of 3,3'-diaminobenzidine (DAB) and 0.00075% H<sub>2</sub>O<sub>2</sub> for 30 minutes at room temperature, yielding a brown reaction product.<sup>4</sup> Control sections were treated only with 0.75 mg/mL of DAB in 0.00075% H<sub>2</sub>O<sub>2</sub>. Because the DAB reaction product is brown, some sections were bleached by incubation overnight in 3% H<sub>2</sub>O<sub>2</sub> prior to Perls Prussian blue staining to improve visibility of the Perls signal in pigmented RPE cells. Sections were counterstained with methylene blue/azure II (Richardson stain) or with periodic acid-Schiff (PAS)-hematoxylin.

Sections were analyzed by brightfield and fluorescence microscopy (using the model TE-300 microscope; Nikon, Tokyo, Japan). The RPE and Bruch's membrane were differentiated based on their unique characteristics using PAS-hematoxylin stain and using autofluorescence.

### IRON CHELATION

To distinguish between chelatable and nonchelatable pools of iron, sections were iron chelated prior to Perls Prussian blue staining by incubation in 0.1M deferoxamine (Sigma-Aldrich Corp, St Louis, Mo) for 24 hours at 37°C.

### DATA ANALYSIS

In unbleached sections, the total iron concentration was assessed by the increase in brown reaction product in Perls-DAB-stained sections compared with control sections. Because we observed no difference between unstained sections and sections treated with DAB/H<sub>2</sub>O<sub>2</sub> only, unstained sections were used as controls. Prior chelation with deferoxamine resolved total iron concentrations into chelatable and nonchelatable forms. Chelatable iron was assessed by comparing Perls-DAB label in nonchelated sections with label in adjacent chelated sections; nonchelatable iron was assessed by comparing chelated sections with adjacent unstained sections. Adjacent sections were stained with PAS-hematoxylin for histologic reference.

Digitized 36-bit red/green/blue images were taken from the region of nonchelated maculas, both healthy and AMD affected, with the highest levels of Perls-DAB signal using a microscope and a Spot RT Slider camera (Diagnostic Instruments, Standish, England). These areas were selected by viewing sections spanning the optic nerve, macula, and retina just temporal to the macula. For each case, several areas that subjectively had the highest levels of Perls signal were selected for digital analysis. The area with the highest Perls signal by quantification of digital images was used for comparison with other cases. Equivalent areas from 2 adjacent sections, one chelated before labeling with Perls Prussian blue stain, and the other left unstained, were then imaged using the same exposure parameters as for the nonchelated sections. To facilitate quantification of Perls label, 36-bit red/green/blue images were converted to 12-bit monochrome images and analyzed using ImagePro Plus software, Version 4.1 (Media Cybernetics, Silver Spring, Md). Retinal pigment epithelium and Bruch's membrane were precisely outlined, and the mean pixel density of the RPE and Bruch's membrane was measured to estimate the total brown stain, consisting of the DAB reaction product and endogenous melanin pigment. Because equivalent areas in adjacent sections should not demonstrate significant variability in endogenous pigment, differences in pixel density between adjacent sections were used to calculate relative levels of chelatable, nonchelatable, and total iron concentrations as described earlier. The Wilcoxon rank sum test was used to compare total iron concentrations in AMD-affected vs healthy maculas.

## RESULTS

### IRON ACCUMULATION IN AMD-AFFECTED EYES

Initial evaluation of iron concentrations in AMD-affected vs healthy maculas used bleached sections to remove endogenous melanin in the RPE. Seven healthy maculas and 8 AMD-affected maculas (1 with early AMD, 5 with GA, and 2 with exudative AMD) were bleached as necessary, Perls Prussian blue stained, and analyzed. These sections were compared with adjacent unstained and DAB/H<sub>2</sub>O<sub>2</sub>-only control sections. The bleached sections were ideal for preliminary assessment of increased iron concentration, but the bleaching process disrupted the morphology. Adjacent, unbleached sections stained with PAS-hematoxylin and viewed for RPE autofluorescence were used to differentiate between the RPE and Bruch's membrane.

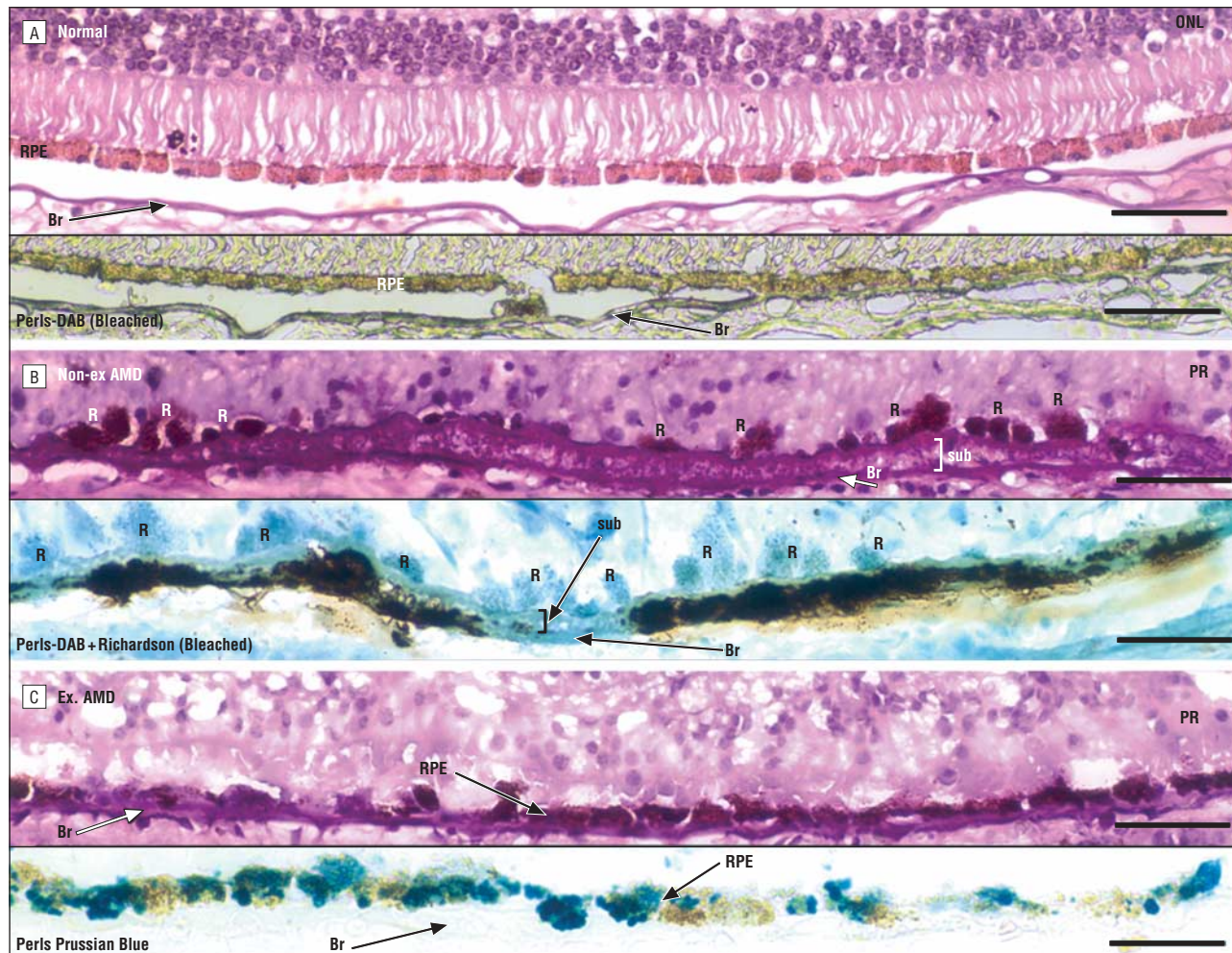


**Figure 1.** Photomicrographs of increased Perls-positive iron in age-related macular degeneration (AMD)-affected retinas compared with healthy retinas. Insets show Perls Prussian blue-stained retinal pigment epithelium (RPE) and Bruch's membrane (Br) in the same region as the larger figure of an adjacent periodic acid-Schiff (PAS)-hematoxylin-stained section. The PAS-hematoxylin-stained sections were unbleached, while sections shown in the insets were bleached as indicated. ONL indicates outer nuclear layer; PR, disorganized photoreceptors. A, Healthy macula has no Perls-3,3'-diaminobenzidine (DAB) stain after bleaching (inset). The remaining melanin in the RPE is identical to the DAB-hydrogen peroxide-only control (not shown), consisting of incompletely bleached endogenous RPE and not Perls-DAB signal. B, Nonexudative (Non-ex) AMD-affected, geographic atrophic macula with severe photoreceptor loss, RPE atrophy, and sub-RPE deposits. Bruch's membrane and sub-RPE deposits (sub) are positive for iron (inset). The RPE cells are unpigmented because endogenous RPE melanin has been bleached, but the Richardson (methylene blue/azure II) counterstain identifies RPE cells (Rs). C, Exudative AMD-affected retina adjacent to a fibrovascular scar in the macula. There is severe photoreceptor loss with RPE atrophy and thickened BR. The RPE contains iron detectable by the Perls Prussian blue stain without DAB enhancement (inset). Scale bars indicate 50  $\mu$ m.

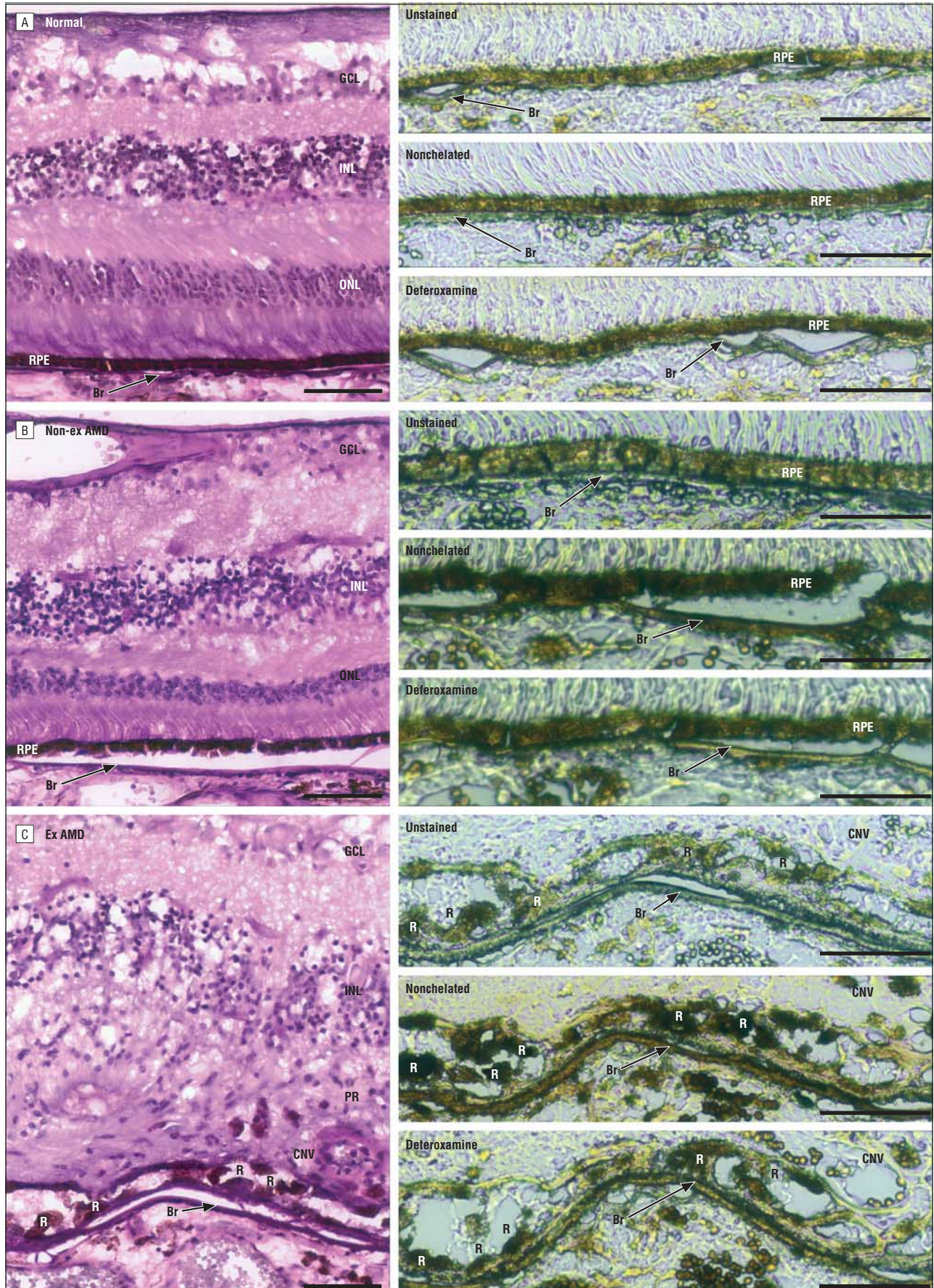
In this initial survey, all DAB/H<sub>2</sub>O<sub>2</sub>-only control sections from healthy and AMD-affected maculas had no brown DAB product and were identical to unstained sections (not shown), indicating the specificity of the DAB-enhanced Perls Prussian blue stain. Additionally, healthy maculas had only low levels of the Perls label (**Figure 1A**).

Relative to the healthy maculas, the increased iron concentration was present in the RPE and/or Bruch's membrane (both, in most cases) of all AMD-affected maculas with early AMD, GA, and exudative AMD in our series. Representative images from healthy maculas and AMD-affected maculas (early AMD, GA, and exudative AMD) are shown in Figure 1 and **Figure 2**. For example, in a macula with GA (Figure 1B), within a region of extensive RPE atrophy and severe photoreceptor loss and disorganization, focal accumulations of iron were observed in the substantially thickened Bruch's membrane and sub-RPE deposits (inset, Figure 1B). While it was necessary to use

Perls-DAB to detect iron in most AMD-affected eyes, iron in an exudative AMD retina with a large macular fibrovascular scar was detectable without enhancement as a Prussian blue reaction product in an area temporal to the macula (Figure 1C). This blue Perls signal was present in the RPE (inset, Figure 1C) in an area with photoreceptor loss but a normal-appearing Bruch's membrane. Although iron was increased primarily in areas of pathologic abnormality (exemplified in Figure 1B,C), an increased iron concentration was also occasionally observed in AMD-affected maculas in areas with nearly normal morphology (Figure 2B).

#### CHELATABLE AND NONCHELATABLE IRON ARE PRESENT IN AMD

To further evaluate iron within the RPE and Bruch's membrane, we analyzed unbleached, Perls Prussian



blue-stained maculas composed of 9 healthy and 10 AMD-affected eyes (3 with early AMD, 3 with GA, and 4 with exudative AMD) with intact morphology. In all Perls Prussian blue-stained sections, red blood cells were positive for Perls label, reflecting the presence of iron-containing heme. Previous studies on iron overload in postmortem brains from patients with Alzheimer disease have used tissue iron chelation with deferoxamine to decrease tissue iron prior to Perls labeling to help validate the specificity of Perls-labeling signal.<sup>4</sup> Because deferoxamine can remove iron from low-molecular-weight complexes as well as from the iron storage protein ferritin,<sup>6</sup> we used deferoxamine in this study both as a negative control for the Perls technique and to determine which portion of the iron pool is in low-molecular-weight complexes or ferritin, as opposed to nonchelatable forms such as in heme.

As shown in a representative healthy macula (Figure 2A), differences in Perls-DAB stain in RPE and Bruch's membrane among unstained, nonchelated, and chelated sections were small, confirming accumulation of only low concentrations of iron within most healthy maculas. One of 9 healthy maculas had a weak Perls signal in focal patches of Bruch's membrane. In contrast, all AMD-affected maculas (3 with early AMD, 3 with GA, 4 with exudative AMD) had increased iron concentrations in the RPE relative to healthy retinas. Eight of 10 AMD-affected maculas also had increased iron concentrations in Bruch's membrane. Increased total iron concentrations in both the RPE and Bruch's membrane constituted both chelatable and nonchelatable forms. In a nonexudative macula with soft drusen and mild photoreceptor loss, consistent with early AMD (Figure 2B), a representative increase in the iron concentration was present throughout the RPE and Bruch's membrane. The increased iron concentration was observed in the nonchelated section compared with the unstained section (total iron), in the nonchelated section compared with the chelated section (chelatable iron), and in the chelated section compared with the unstained section (nonchelatable iron). In an exudative AMD-affected macula (Figure 2C), iron had accumulated in an area of severe pathologic abnormality with extensive photoreceptor loss and

disorganization, fibrovascular scarring, choroidal neovascularization, and RPE disruption with a thickened Bruch's membrane and sub-RPE deposits. Both chelatable and nonchelatable iron were increased in the RPE and Bruch's membrane of this exudative AMD-affected macula.

Because of the obscuring endogenous RPE melanin of these unbleached sections, some changes in iron in the RPE and Bruch's membrane were subtle. To quantify differences in iron levels and to determine whether AMD-affected maculas had statistically significantly increased Perls-detectable iron, panels of 4 sections (unstained, nonchelated, chelated, and PAS stained) were compared from 10 AMD-affected maculas (3 with early AMD, 3 with GA, and 4 with exudative AMD) and 9 healthy control maculas. By selecting areas with the highest Perls signal from each macula and comparing pixel densities between the same regions from adjacent unstained sections and sections treated with Perls label, or deferoxamine followed by Perls label, relative levels of total, chelatable, and nonchelatable iron were estimated.

**Figure 3** shows that compared with healthy maculas, AMD-affected maculas have an increased total Perls-DAB signal in the RPE (mean [SEM] values, 1372 [84] vs 262 [79] arbitrary units) and Bruch's membrane (mean [SEM] values, 864 [117] vs 149 [50] arbitrary units). These increases are statistically significant by the Wilcoxon rank sum test, with  $P < .001$  for RPE and  $P = .001$  for Bruch's membrane. Iron in the RPE and Bruch's membrane of AMD-affected maculas was partially chelatable, as indicated by the solid bars in Figure 3.

## COMMENT

Iron is a critical element in human metabolism but also a potent source of highly reactive hydroxyl free radicals via the Fenton reaction. Free iron is normally maintained at low levels by tight regulatory mechanisms to prevent ensuing oxidative damage. There is growing evidence that neurodegenerative diseases, including AMD and Alzheimer disease, are induced by increased oxidative stress and free radical damage.<sup>2,3,7</sup> Recent studies demonstrated increased iron concentrations in senile plaques and neurofibrillary tangles, implicating iron-mediated oxidative damage in the pathogenesis of Alzheimer disease.<sup>4</sup> To investigate whether iron might be involved in the pathogenesis of AMD, we analyzed iron distribution in AMD-affected maculas compared with healthy maculas. We found that maculas with early AMD, GA, and exudative AMD had increased iron in the RPE and Bruch's membrane compared with healthy maculas.

While iron itself has not previously been implicated in the pathogenesis of AMD, there is evidence of altered iron metabolism in AMD-affected maculas. Heme oxygenase-1 and -2 are increased in RPE of AMD-affected maculas.<sup>8</sup> Heme oxygenase is an antioxidant protein that mediates the release of iron from heme-containing proteins, and an increase in heme oxygenase may result in increased iron deposition. Most recently,  $\beta$ -amyloid, a component of senile plaques and a pathologic hallmark of Alzheimer disease,<sup>9</sup> was detected in drusen.<sup>10</sup>  $\beta$ -Amyloid has a high affinity for iron, and toxic effects of  $\beta$ -amyloid in Alzheimer disease may result from its bound iron.<sup>9,11</sup>

**Figure 2.** Photomicrographs of chelatable and nonchelatable iron accumulation in unbleached age-related macular degeneration (AMD)-affected maculas but not healthy maculas. Large panels show maculas stained with periodic acid-Schiff (PAS)-hematoxylin, and insets show adjacent sections unstained or stained with Perls-3,3'-diaminobenzidine (DAB) with or without prior deferoxamine chelation. ONL indicates outer nuclear layer; INL, inner nuclear layer; GCL, ganglion cell layer; CNV, choroidal neovascularization. Note that red blood cells are positive for Perls-DAB stain, as expected. A, Healthy macula with minimal Perls-DAB signal observed in the retinal pigment epithelium (RPE) or Bruch's membrane (Br) of either the chelated or nonchelated sections, which appear only slightly darker than the unstained section. B, Nonexudative AMD-affected macula with signs of early AMD including drusen (not shown), slightly thickened Br, and mild photoreceptor (PR) loss without RPE atrophy. The RPE and Br in the nonchelated section are darker than in the unstained section, owing to increased Perls-DAB stain corresponding to total iron accumulation. Some of the increased iron is chelatable, demonstrated by decreased Perls-DAB stain in the deferoxamine-chelated compared with the nonchelated section. C, Exudative AMD-affected macula with marked PR loss, fibrovascular scarring, sub-RPE deposits, and thickened Br. Choroidal neovascularization is present, with the same vessel in all sections, and few RPE cells (Rs) remain. Iron is increased in the RPE cells and Br and consists of both chelatable and nonchelatable forms. Scale bars indicate 50  $\mu$ m.

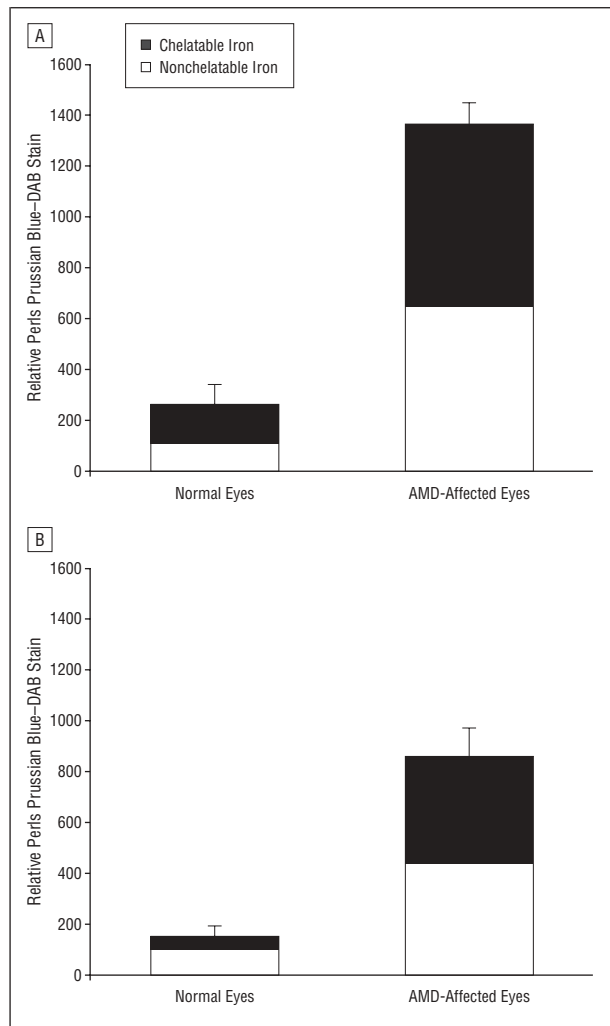


**Figure 3.** Bar graphs of increased iron in age-related macular degeneration (AMD) vs healthy maculas. Iron levels were estimated by calculating differences in Peris Prussian blue stain intensity (measured as pixel density) between adjacent sections from 10 AMD-affected maculas (3 with drusen only, 3 with geographic atrophy, and 4 with exudative AMD) and from 9 healthy eyes, as described in the “Methods” section. The AMD-affected maculas have statistically significantly increased total iron concentrations (bar height  $\pm$  SEM) in retinal pigment epithelium (A) and Bruch’s membrane (B) compared with healthy eyes,  $P < .001$  for retinal pigment epithelium and  $P = .001$  for Bruch’s membrane. Some of this iron is chelatable (solid bars) while the remainder is nonchelatable (open bars). DAB indicates 3,3’-diaminobenzidine.

The presence of  $\beta$ -amyloid in the drusen of AMD-affected eyes might similarly cause retinal degeneration by increased iron-mediated oxidative damage.

The toxic effects of iron in the eye are well established. In siderosis bulbi from an iron foreign body retained in the eye, or after experimental injection of iron into the vitreous, progressive iron deposition throughout the eye causes photoreceptor degeneration.<sup>12-14</sup> In models of subretinal hemorrhage, the ensuing photoreceptor degeneration is believed to result, at least in part, from the toxic effects of iron.<sup>15</sup> Royal College of Surgeons rats have increased RPE and photoreceptor iron compared with controls, which may contribute to their retinal degeneration.<sup>16</sup>

The cause of iron accumulation in AMD most likely involves abnormal iron transport and storage. Photore-

ceptor inner and outer segments maintain relatively high iron levels necessary to meet requirements for metabolic processes including oxidative phosphorylation and membrane biogenesis.<sup>16</sup> Because photoreceptor outer segments are shed and phagocytosed by RPE, a mechanism for returning iron to photoreceptors must exist. In vitro evidence suggests that RPE cells may take up iron from the choriocapillaris and transfer it to photoreceptors.<sup>17</sup> Dysfunction of any step in this iron transport process could lead to iron overload. As a model of such dysfunction, mice with mutations in 2 ferroxidases—ceruloplasmin and hephaestin—that facilitate cellular iron export in other cell types,<sup>18,19</sup> accumulate large amounts of RPE iron (Zena Leah Harris, MD, and P.H. and J.L.D, unpublished data, 2003). Similarly, patients who have aceruloplasminemia also have retinal degeneration with RPE atrophy,<sup>20,21</sup> and the retinal degeneration in patients lacking this ferroxidase may reflect intracellular accumulation of iron. Accumulations of metal-binding proteins such as  $\beta$ -amyloid could also result in iron overload.

Our finding that AMD-affected maculas have increased iron concentrations suggests that retinal degeneration in AMD might be related to iron-mediated oxidative stress. Iron is increased in early AMD, suggesting that iron overload may be involved in the early pathogenesis of AMD rather than a result of late events in the disease process. Also in support of this hypothesis, iron is increased in relatively healthy regions of some AMD maculas. Iron in AMD-affected maculas varied from focal to diffuse and was observed in the RPE and Bruch’s membrane. Prior histopathologic studies suggest that RPE atrophy precedes photoreceptor degeneration in AMD,<sup>22,23</sup> and it is possible that iron accumulation within the RPE and Bruch’s membrane causes RPE damage and death, with secondary photoreceptor degeneration.

We were unable to distinguish between different oxidation states of iron. Further studies using fresh frozen tissues or fixatives such as methacarn that better preserve the redox states of iron<sup>4</sup> are needed to assess the relative concentrations of ferric and ferrous iron.

## CONCLUSIONS

Our novel finding of increased iron in AMD-affected maculas implicates iron-mediated oxidative damage in the pathogenesis of AMD and warrants investigation of iron chelation as potential therapy. We found that some of the iron in the RPE and Bruch’s membrane was chelatable with deferoxamine. Iron chelation therapy might decrease abnormally high iron levels in AMD-affected maculas and thereby lessen oxidative stress in RPE cells. However, it is not yet known whether reversing iron deposition at any stage of the disease will alter the clinical outcome, necessitating further investigation of the mechanisms of normal iron transport in the retina and the role of iron in AMD pathogenesis.

Submitted for publication October 14, 2002; final revision received March 27, 2003; accepted April 8, 2003.

This study was supported in part by funds from the Research to Prevent Blindness Career Development Award; International Retina Research Foundation; grant EY00417 from

the National Institutes of Health, Bethesda, Md; Foundation Fighting Blindness, Owings Mills, Md; Fight for Sight, London, England; Pennsylvania Lions Foundation, Philadelphia; McCabe Fund, Philadelphia; Mackall Trust, Philadelphia.

We thank Gui-Shuang Ying, MS, and Maureen G. Maguire, PhD, for statistical consultation, Waixing Tang, MD, and Julie Smith for technical assistance, Joan Fisher for coordinating the eye donations, and the late Jeffrey W. Berger, MD, PhD, for helpful discussions.

Corresponding author and reprints: Joshua L. Dunaeief, MD, PhD, F. M. Kirby Center for Molecular Ophthalmology, Scheie Eye Institute, University of Pennsylvania, 305 Stellar Chance Laboratories, Philadelphia, PA 19104 (e-mail: jdunaeief@mail.med.upenn.edu).

## REFERENCES

1. Klein R, Wang Q, Klein BE, Moss SE, Meuer SM. The relationship of age-related maculopathy, cataract, and glaucoma to visual acuity. *Invest Ophthalmol Vis Sci.* 1995;36:182-191.
2. Beatty S, Koh H, Phil M, Henson D, Boulton M. The role of oxidative stress in the pathogenesis of age-related macular degeneration. *Surv Ophthalmol.* 2000;45:115-134.
3. A randomized, placebo-controlled, clinical trial of high-dose supplementation with vitamins C and E, beta carotene, and zinc for age-related macular degeneration and vision loss: AREDS report No. 8. *Arch Ophthalmol.* 2001;119:1417-1436.
4. Smith MA, Harris PL, Sayre LM, Perry G. Iron accumulation in Alzheimer disease is a source of redox-generated free radicals. *Proc Natl Acad Sci U S A.* 1997;94:9866-9868.
5. Milam AH. Immunocytochemical studies of the retina. In: Rakoczy PE, ed. *Vision Research Protocols.* Totowa, NJ: Humana Press; 2001:71-88. *Methods in Molecular Medicine.* vol 47.
6. Kontoghiorghe GJ, Pattichi K, Hadjigavriel M, Kolnagou A. Transfusional iron overload and chelation therapy with deferoxamine and deferiprone (L1). *Transfus Sci.* 2000;23:211-223.
7. Smith MA, Rottkamp CA, Nunomura A, Raina AK, Perry G. Oxidative stress in Alzheimer's disease. *Biochim Biophys Acta.* 2000;1502:139-144.
8. Frank RN. "Oxidative protector" enzymes in the macular retinal pigment epithelium of aging eyes and eyes with age-related macular degeneration. *Trans Am Ophthalmol Soc.* 1998;96:635-689.
9. Atwood CS, Moir RD, Huang X, et al. Dramatic aggregation of Alzheimer abeta by Cu(II) is induced by conditions representing physiological acidosis. *J Biol Chem.* 1998;273:12817-12826.
10. Johnson LV, Leitner WP, Rivest AJ, Staples MK, Radeke MJ, Anderson DH. The Alzheimer's abeta-peptide is deposited at sites of complement activation in pathologic deposits associated with aging and age-related macular degeneration. *Proc Natl Acad Sci U S A.* 2002;99:11830-11835.
11. Rottkamp CA, Raina AK, Zhu X, et al. Redox-active iron mediates amyloid-beta toxicity. *Free Radic Biol Med.* 2001;30:447-450.
12. Tawara A. Transformation and cytotoxicity of iron in siderosis bulbi. *Invest Ophthalmol Vis Sci.* 1986;27:226-236.
13. Vergara O, Ogden T, Ryan S. Posterior penetrating injury in the rabbit eye: effect of blood and ferrous ions. *Exp Eye Res.* 1989;49:1115-1126.
14. Doly M, Bonhomme B, Vennart JC. Experimental study of the retinal toxicity of hemoglobin iron. *Ophthalmic Res.* 1986;18:21-27.
15. Glatt H, Machermer R. Experimental subretinal hemorrhage in rabbits. *Am J Ophthalmol.* 1982;94:762-773.
16. Yefimova MG, Jeanny JC, Keller N, et al. Impaired retinal iron homeostasis associated with defective phagocytosis in Royal College of Surgeons rats. *Invest Ophthalmol Vis Sci.* 2002;43:537-545.
17. Hunt RC, Davis AA. Release of iron by human retinal pigment epithelial cells. *J Cell Physiol.* 1992;152:102-110.
18. Harris ZL, Durlley AP, Man TK, Gitlin JD. Targeted gene disruption reveals an essential role for ceruloplasmin in cellular iron efflux. *Proc Natl Acad Sci U S A.* 1999;96:10812-10817.
19. Vulpe CD, Kuo YM, Murphy TL, et al. Hephaestin, a ceruloplasmin homologue implicated in intestinal iron transport, is defective in the sla mouse. *Nat Genet.* 1999;21:195-199.
20. Miyajima H, Nishimura Y, Mizoguchi K, Sakamoto M, Shimizu T, Honda N. Familial apoceruloplasmin deficiency associated with blepharospasm and retinal degeneration. *Neurology.* 1987;37:761-767.
21. Morita H, Ikeda S, Yamamoto K, et al. Hereditary ceruloplasmin deficiency with hemosiderosis: a clinicopathological study of a Japanese family. *Ann Neurol.* 1995;37:646-656.
22. Curcio CA, Medeiros NE, Millican CL. Photoreceptor loss in age-related macular degeneration. *Invest Ophthalmol Vis Sci.* 1996;37:1236-1249.
23. Sarks JP, Sarks SH, Killingsworth MC. Evolution of geographic atrophy of the retinal pigment epithelium. *Eye.* 1988;2(pt 5):552-577.

### Notice to Authors: Submission of Manuscripts

Selected manuscripts submitted to the *Archives of Ophthalmology* will be submitted for electronic peer review. Please enclose a diskette with your submission containing the following information:

File name  
Make of computer  
Model number  
Operating system  
Word processing program and version number